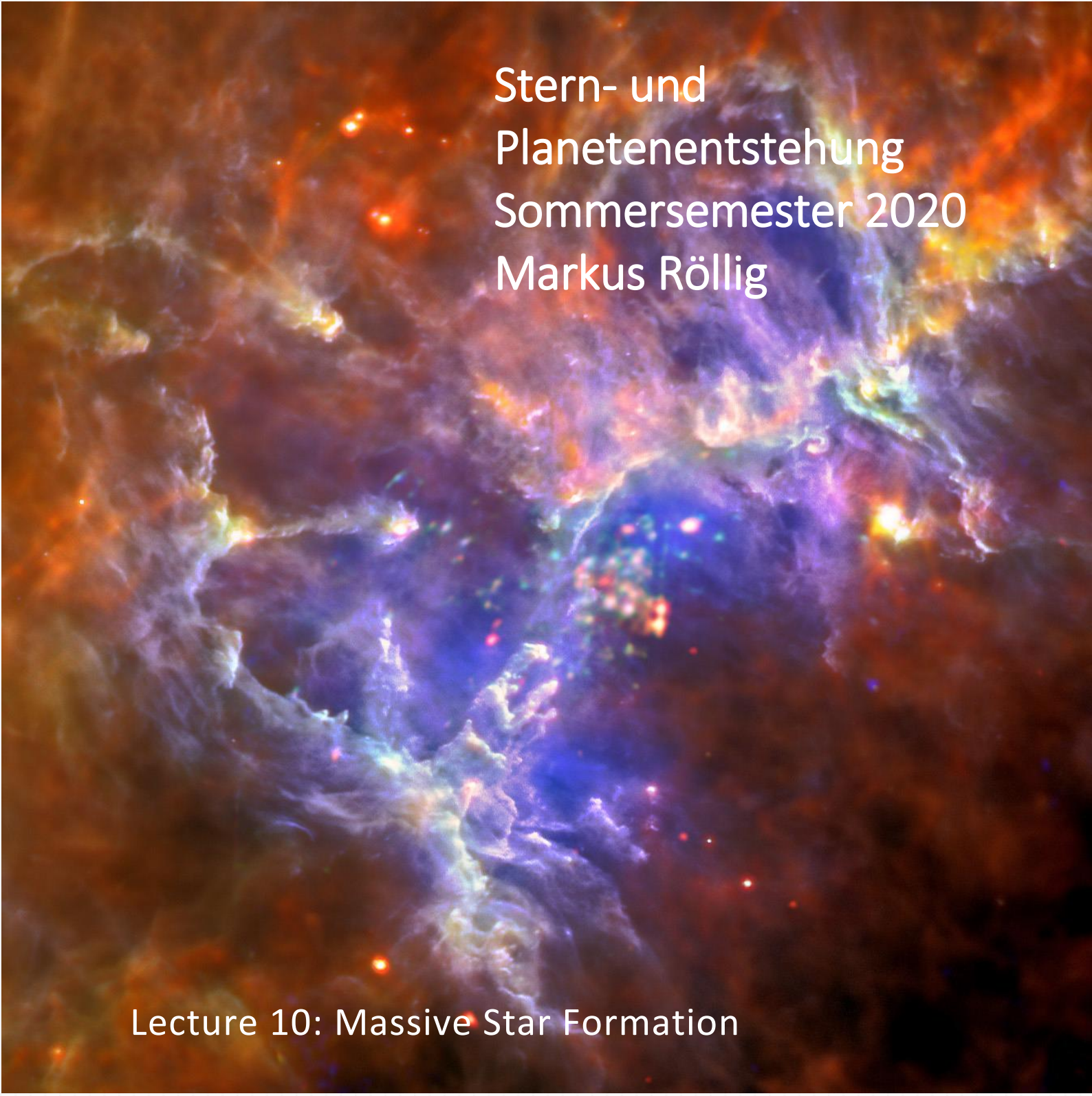

Stern- und Planetenentstehung
Sommersemester 2020
Markus Röllig

Lecture 10: Massive Star Formation

http://exp-astro.physik.uni-frankfurt.de/star_formation/index.php

VORLESUNG/LECTURE

Raum: Physik - 02.201a
dienstags, 12:00 - 14:00 Uhr

SPRECHSTUNDE:

Raum: GSC, 1/34, Tel.: 47433, (roellig@ph1.uni-koeln.de)
dienstags: 14:00-16:00 Uhr

Nr.	Thema	Termin
1	Observing the cold ISM	21.04.2020
2	Observing Young Stars	28.04.2020
3	Gas Flows and Turbulence Magnetic Fields and Magnetized Turbulence	05.05.2020
4	Gravitational Instability and Collapse	12.05.2020
5	Stellar Feedback	19.05.2020
6	Giant Molecular Clouds	26.05.2020
7	Star Formation Rate at Galactic Scales	02.06.2020
8	Stellar Clustering	09.06.2020
9	Initial Mass Function – Observations and Theory	16.06.2020
10	Massive Star Formation	23.06.2020
11	Protostellar disks and outflows – observations and theory	30.06.2020
12	Protostar Formation and Evolution	07.07.2020
13	Late Stage stars and disks – planet formation	14.07.2020

10 Massive Star Formation

Stars with $M > 10M_{\odot}$ constitute 10% of all stellar mass and only 0.2% of their number.

$$L \propto M^{3.5}$$

$$M = 10 \Rightarrow L \sim 3000\, L_{\odot}, M = 20 \Rightarrow L \sim 3.5 \times 10^{4} L_{\odot},$$
$$M = 30 \Rightarrow L \sim 10^{5} L_{\odot}$$

10.1 Observational Phenomenology

10.1.1 Challenges

- Massive stars are rare
  - Closest: Orion cloud (413pc), typical ~2-3kpc
  - compare to low mass SF regions: D~100-150 pc
  - only large spatial scales resolvable
- Crowding & Confusion
  - massive stars found in clusters
  - extreme spatial resolution to avoid confusion
- Obscuration
  - typical Σ for massive SF region ~1 g cm^{-2}
    - $A_V \sim 500, A_K \sim 50$
    - stars deeply embedded
- Time-scales
  - massive SF timescale ~ 10^5yr compared to 10^6 yr of low mass SF
  - massive SF happens while still embedded (no Class II or III phases)

10.1.2 Massive Clumps

Sites of massive SF

- huge far-IR fluxes
- maser emission
  - pumped by shocks (from outflows)
- $\Sigma \sim 0.1 - 1\ \mathrm{g\ cm^{-2}}$
- IRDC (infrared dark clouds)

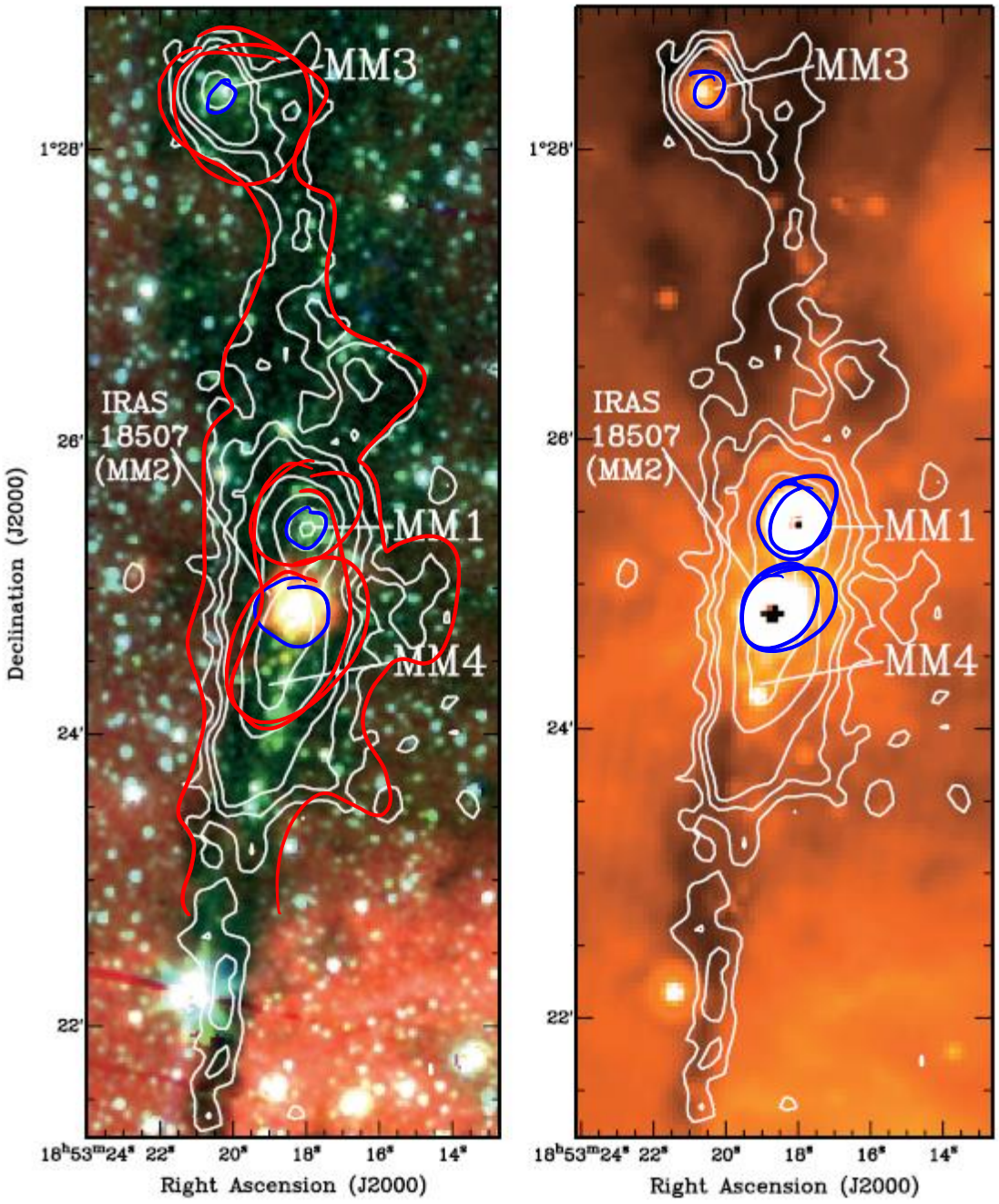

FIG. 1.—G34.4+0.2. *Left*: *Spitzer*/IRAC three-color image (3.6 μm in blue, 4.5 μm in green, and 8.0 μm in red) overlaid with IRAM/MAMBO-II 1.2 mm continuum emission (contour levels 60, 90, 120, 240, 480, 1200, and 2200 mJy beam^{-1}). *Right*: *Spitzer*/MIPS 24 μm image with contours of the IRAM/MAMBO-II 1.2 mm continuum emission (logarithmic color scale, 30 MJy sr^{-1} [*black*] to 200 MJy sr^{-1} [*white*]). Labeled on this figure are the four millimeter cores.

Abbildung 1 Rathborne et al. 2005

- masses ~ few thousand $M_\odot$
- sizes ~ 1-2 pc
- off the linewidth-size relation

10.1.3 Massive Cores

Zooming in:

- ~ 0.1 pc
- objects of $M \approx 100\ M_\odot$
- centrally concentrated
- forming stars
- $\sigma \approx 1\ \mathrm{km\ s^{-1}}$
- off the linewidth-size relation
- starless phase of a massive core ~1000 yr
- $M = 100\ M_\odot\ , R = 0.1\ \mathrm{pc} \Rightarrow n = 10^6\ (10^{18} \mathrm{g\ cm^{-3}}), t_{ff} = 5 \times 10^4 \mathrm{yr}$
- $\Rightarrow \dot{M} \approx \frac{M}{t_{ff}} \approx 10^{-3} M_\odot \mathrm{yr}^{-1}$ (much higher compared to low M SF)

$$\alpha_{vir} = \frac{5\sigma^2 R}{GM} \approx 1$$

$$t_{ff} = \sqrt{\frac{3\pi}{32 g\rho}} = \sqrt{\frac{\pi R^3}{8GM}}$$

$$\dot{M} \approx \frac{M}{t_{ff}} = \sqrt{\frac{8GM^3}{\pi R^3}} = \sqrt{\frac{1000}{\pi \alpha_{vir}^3}} \frac{\sigma^3}{G} \approx \frac{10\sigma^3}{G}$$

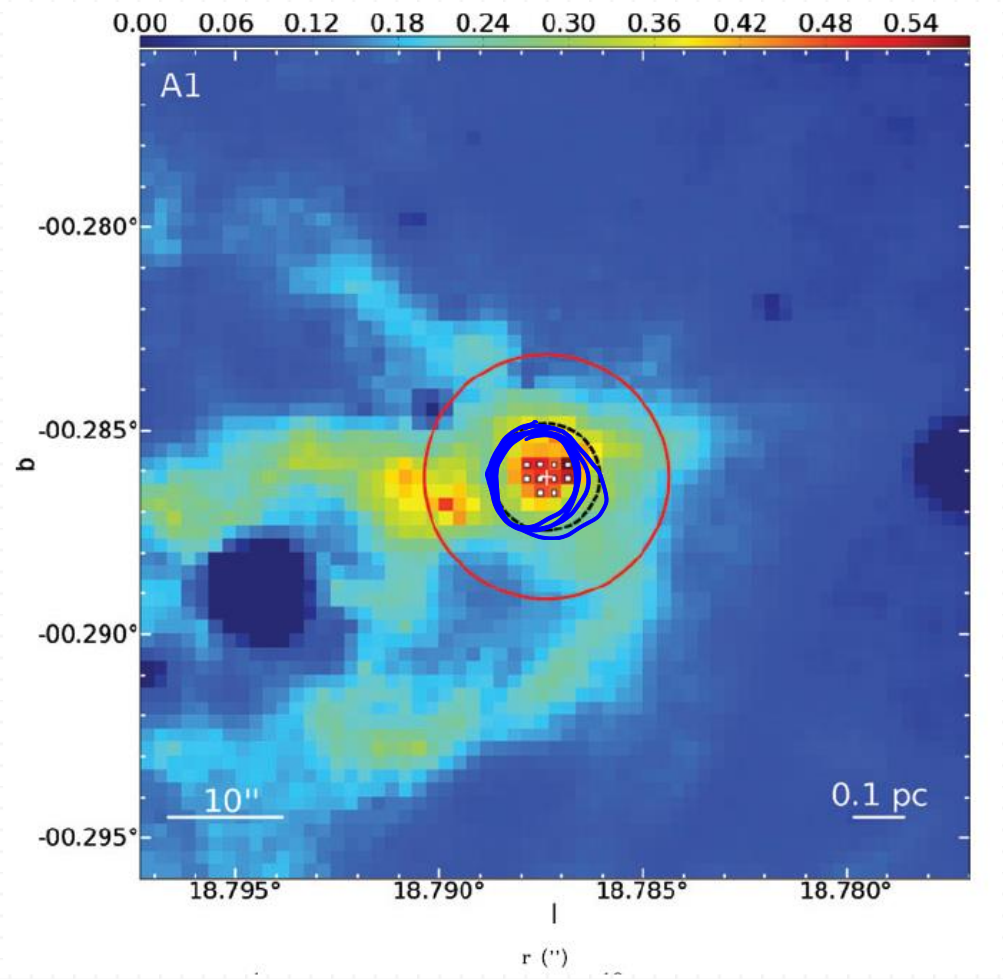

Abbildung 2 A massive protostellar core seen in IR absorption (Butler & Tan, 2012). Colors indicate the inferred column density in g cm^{-2}. Pixels marked with white dots are lower limits. The black circle shows a radius enclosing 60 $M_\odot$ and the red circle shows the core radius inferred by fitting a core plus envelope model to the azimuthally-averaged surface density distribution.

10.2 FRAGMENTATION

10.2.1 Massive Core Fragmentation

$$M_J = 26 M_\odot \left(\frac{T}{10K}\right)^{\frac{3}{2}} \left(\frac{n}{10^3 cm^{-3}}\right)^{-1/2}$$

@10K and 10^6cm^{-3} M_J<1solar mass

⇨ massive cores fragment

combination of magnetic fields and radiative heating can suppress fragmentation (Commercon et al 2011, Myers et al. 2013)

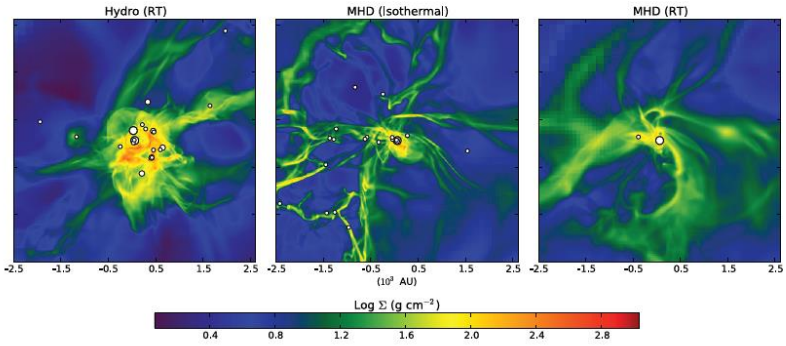

Figure 14.3: Three simulations of the collapse of a 300 $M_\odot$ massive core by Myers et al. (2013). The color scale shows the projected gas density, and white points are stars, with the size indicating the mass. The three simulations use identical initial conditions, but different physics. The left panel uses radiative transfer but no magnetic fields, the middle uses magnetic fields but no radiation, and the right panel includes both magnetic fields and radiation.

- rapid accretion
- high accretion luminosity
- strong gas heating
- Jean's mass increases
- magnetic fields increase accretion rate (by transporting angular momentum)
- magnetic fields stabilize cooler parts against fragmentation

10.2.2 Massive Binaries

Binaries can form in two ways:

- direct fragmentation (during collapse)
  - produces wide binaries
- disk fragmentation
- fragmentation depends on level of initial turbulence
- time of fragmentation controlled
  - by rate of rotation
  - strength of magnetic fields
  - gas density and temperature

10.3 Barriers to Accretion

10.3.1 Evolution of a Massive Protostar

- Formation time ~ 10^5 yr
- Kelvin time $t_{KH} = \frac{GM^2}{RL}$
  - ~20 kyr for a 50 $M_\odot$ ZAMS star

- star reaches equilibrium (main sequence, i.e. nuclear fusion in the center stated) while still accreting
- rapid contraction produces very strong winds

10.3.2 Winds

Do the strong winds inhibit further accretion?

Wind speed ~1000 km s^{-1} $\dot{M}_{wind} \approx 10^{-7} M_{\odot} yr^{-1}$

mass flux $\dot{M} = 4\pi r^2 \rho v$ ram pressure $P_{wind} = \rho v^2 = \frac{\dot{M}_{wind} v_{wind}}{4\pi r^2}$

accretion mass flux ~$10^{-4} - 10^{-3} M_{\odot} yr^{-1}$

infall ram pressure $P_{infall} = \frac{\dot{M}_{infall} v_{ff}}{4\pi r^2}$

$$\frac{P_{infall}}{P_{wind}} = \frac{\dot{M}_{acc} v_{ff}}{\dot{M}_{wind} v_{wind}}$$

velocities about equal, therefore infalling matter can stop the wind

10.3.3 Ionization

Can the radiation stop accretion?

- photons with $E > 13.6\ eV$ can ionize hydrogen
- H^+ is heated up to ~ 10 km s^{-1}, sufficient to escape
- but radiation is trapped within a few stellar radii
- here the escape velocity is about 1000 km s^{-1}
- radiation might leak out if core is porous

Qualitatively, the result is that, at the accretion rates that we expect in massive cores, we expect the ionizing radiation to all be trapped within a few stellar radii.

Thus, ionization is an important feedback, but it is one that is likely most important after the massive star has gathered most of the mass around it and has stopped growing

10.3.4 Radiation Pressure

By far the biggest potential worry for massive star formation is not that ionizing radiation will heat the gas enough to allow it to escape, but the pressure exerted by radiation will halt accretion

DUST DESTRUCTION FRONT

dust destruction radius around protostar where all starlight is absorbed

$$\frac{L_*}{4\pi r_d^2}\,\pi a^2 = 4\pi a^2 \sigma T_d^4$$

$$r_d = \sqrt{\frac{L_*}{16\pi\sigma T_d^4}} = 25\ AU\ L_{*,5}^{1/2} T_{d.3}^{-2}$$

Compare the force exerted by the radiation:

- At r_d: radiation still has stellar spectrum.
- Beyond r_d: radiation still gets converted to IR by dust absorption

At a thin shell around r_d all radiation is absorbed (all momentum transferred to the gas).
Infall will reverse if this change in momentum is enough to reduce the infall velocity to zero.

Compare infalling momentum and radiation momentum

$$\dot{p} = -\dot{M}v$$

$$\dot{p} = \frac{L}{c}$$

v_0: velocity just before matter encounters the radiation
v_1: velocity just after

$$\dot{M}v_1 = \dot{M}v_0 - \frac{L}{c}$$

v_1<0 (i.e. still falling inward) requires that

$$\dot{M}v_0 > \frac{L}{c}$$

assume free-fall ($v_0 = \sqrt{2GM/r_d}$)

$$\dot{M} > \frac{L}{v_0 c} = \frac{L}{c}\sqrt{\frac{r_d}{2GM_*}} = 8 \times 10^{-5} M_\odot yr^{-1} L_{*,5}^{3/2} T_{d,3}^{-1} M_{*,1}^{-1/2}$$

Matter will most likely not be stopped at the destruction front

THE ENVELOPE

Radiation must escape the envelope

Radiation flux: $F = L/(4\pi r^2)$

Applied force on **gas**: $f_{rad} = \frac{1}{c}\int \kappa_\nu F_\nu d\nu = \frac{1}{4\pi r^2 c}\int \kappa_\nu L_\nu d\nu$

Rosseland mean oppacity κ_R

$$f_{rad} = \frac{\kappa_R F}{c} = \frac{\kappa_R L_*}{4\pi r^2 c}$$

Force is smaller than at dust destruction front but acts on all radii (not only r_d, and over a long time)

Comparing this force with the gravitational force gives (gravitational force to be stronger than radiative force means > instead of =):

$$\frac{L_*}{M_*} = \frac{4\pi G c}{\kappa_R}$$

$$\left(\frac{L_*}{M_*}\right) = 1300\left(\frac{L_\odot}{M_\odot}\right)\kappa_{R,1}^{-1}$$

Comparison: $50\ M_\odot$ ZAMS star has $\left(\frac{L_*}{M_*}\right) \approx 7100\left(\frac{L_\odot}{M_\odot}\right)$

All stars with $M > 20\ M_{\odot}$ should have a net acceleration outward and therefore be unable to form!

Solution: spherical symmetry does not occur

Accretion will continue as long as there are significant patches of solid angle where gravity wins.

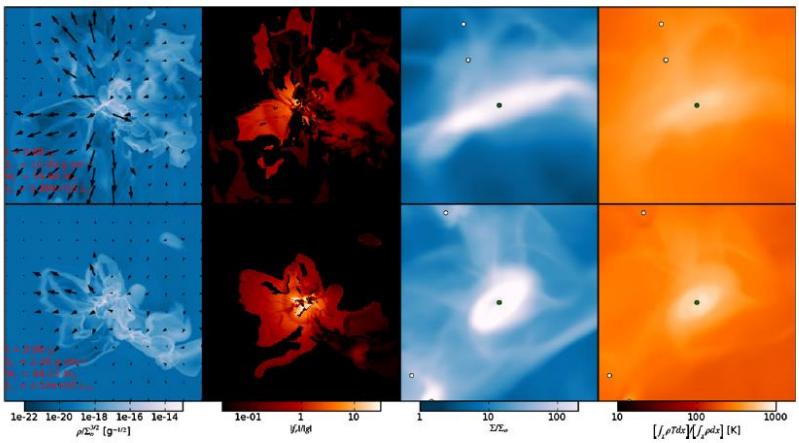

Figure 14.5: Two simulations of the formation of a massive star including protostellar outflows (Cunningham et al., 2011). The top row shows a simulation with an outflow, while the lower shows one without. The panels show, from left to right, normalized volume density in a slice, ratio of radiation force to gravitational force, normalized projected density, and mass-weighted mean projected temperature. Note the general absence of regions with radiation force greater than gravitational force in the simulation with winds.